J Therm Anal Calorim (2015) 121:579–588
DOI 10.1007/s10973-015-4633-x

Study of the hydration of calcium zirconium aluminate ($Ca_7ZrAl_6O_{18}$) blended with reactive alumina by calorimetry, thermogravimetry and other methods

Dominika Madej[1] · **Jacek Szczerba**[1]

Received: 5 January 2015 / Accepted: 7 March 2015 / Published online: 19 March 2015

Abstract The reactivities of hydratable alumina, calcium zirconium aluminate and their binary mixtures were investigated by calorimetric method, X-ray diffraction, Fourier transform infrared spectroscopy (FT-IR), differential thermal/thermogravimetric analysis (DTA–TG) and scanning electron microscope observations. The rate of heat evolution illustrates only one distinct exothermic peak in the mixtures containing calcium zirconium aluminate which corresponds the subsequent precipitation of hydrated material mainly in the form of amorphous $CaO–Al_2O_3–H_2O$ phases and crystalline C_4AH_{19} occurs simultaneously after wetting of $Ca_7ZrAl_6O_{18}$ grains. Nevertheless, coexistence of both unstable calcium aluminate hydrates (CAH_{10}, C_2AH_8, C_4AH_{19}) and thermodynamically more stable C_3AH_6 detected by FT-IR and DTA–TG in the paste cured at 20 °C may have originated in the thermally induced partial conversion reaction due to the considerable amount of heat generated by the $Ca_7ZrAl_6O_{18}$ hydration. It is also found that curing temperature affected the hydration products formed in the hydration products of both $Ca_7ZrAl_6O_{18}$ and $Ca_7ZrAl_6O_{18}/Al_2O_3$ blends. Reactive alumina influences the hydration behavior of $Ca_7ZrAl_6O_{18}$ facilitating the nucleation and growth of hydration products, causes characteristic changes in the microstructure of hardened blended pastes and favors recrystallization of dehydrated calcium aluminates.

✉ Dominika Madej
dmadej@agh.edu.pl

[1] Faculty of Materials Science and Ceramics, AGH University of Science and Technology, 30 Mickiewicza Av., 30-059 Kraków, Poland

Keywords $Ca_7ZrAl_6O_{18}$ · Hydration · Thermal analysis · Calorimetric methods · Hydraulic binder · Reactive alumina micropowder

Introduction

Hydraulic bonding via calcium aluminate cement (CAC) is the most applied mechanism due to both castable fluidity and green mechanical strength [1–5]. Nevertheless, several different alternative bonding systems for monolithic refractories have been developed in recent years mainly due to the necessity of the reduction in CaO content and thereby improve cold and hot strength, reduce porosity, increase density and corrosion resistance of castables [6–8]. At present, special emphasis is put on the preparation and application of reactive alumina able of forming hydrated phases in water, as an alternative hydraulic binder in unshaped refractory materials [9, 10]. Hydraulic alumina powders are widely prepared starting from Bayer gibbsite (α-aluminum hydroxide) via three steps; the reduction in the soda content, heat treatment and particle size reduction in an attritor ball mill [9]. Utility properties of reactive alumina are generally determined by the chemistry, especially by the soda content, primary crystal size, specific surface area (BET) and particle size distribution (mono-/bi-/multimodal). When it is in contact with water, it is gradually converted to bayerite polymorph of $Al(OH)_3$ [10]. Incomplete reaction was found due to the differences in microstructure of hydratable alumina grains.

Besides, many chemical additives may be added to the refractory castables, e.g., to control the hydration process (accelerators/retarders) [11]. For example, Li^+ salts and alkali or calcium hydroxides are considered to be strong accelerators [12]. Nevertheless, many accelerators have a

negative effect on the properties of certain refractories that are applied in high-temperature and highly corrosive environments [13]. These disadvantages can be overcome by using a water-reactive substance chemically similar to the major compounds of CAC. In view of this state of affairs, the major thrust in development of superior cementitious systems is based on the combination of very fine particles of refractory oxides, e.g., reactive alumina micropowder, with other components tailored specifically for this purpose. In our previous works [14–17], we have investigated a hydratable compound, i.e., calcium zirconium aluminate with chemical formula of $Ca_7ZrAl_6O_{18}$. It has a distinctly similar mechanism of hydration when compared to CAC, especially in terms of the C–A–H phases formed in hydrated cement paste. Calcium zirconium aluminate, $Ca_7ZrAl_6O_{18}$, hydrates and hardens very quickly comparable to tricalcium aluminate, $Ca_3Al_2O_6$ [18]. It liberates a large amount of heat almost immediately after mixing with water [14]. Hence, it may be used in high-temperature applications, especially as an additive in mass corundum castables, where it can help to shorten the setting time, or to accelerate the hardening process. An additional benefit of using $Ca_7ZrAl_6O_{18}$ would be the improvement of physical and chemical properties of refractory castables due to the formation of calcium zirconate, $CaZrO_3$, characterized by high melting point, low thermal expansion coefficient, high strength and excellent corrosion resistance against alkali oxides [14, 19]. In this paper, we propose and investigate the hydration processes of new binder based on the hydratable materials: calcium zirconium aluminate and reactive alumina as a new cementitious system for the technology of monolithic refractories.

Experimental

Synthesis procedure of calcium zirconium aluminate ($Ca_7ZrAl_6O_{18}$)

The subject of the study was hardened $Ca_7ZrA_6O_{18}$ and reactive alumina/$Ca_7ZrA_6O_{18}$ pastes prepared with water/solid ratio of 0.5 and cured up to 32 days under different curing temperatures. Calcium zirconium aluminate, $Ca_7ZrAl_6O_{18}$, was synthesized by high-temperature solid-state method. For a typical synthesis, stoichiometric amounts calcium carbonate (98.81 % $CaCO_3$, Chempur), aluminum oxide (99.7 % Al_2O_3, Chempur) and zirconium dioxide (98.08 % ZrO_2, Merck) were mixed for 2 h in a ball mill to obtain a homogeneous mixture. The mixture was then shaped in the form of cylindrical specimens (diameter 20 mm, height 20 mm) and calcined at 1200 °C for 10 h in an air atmosphere electric furnace. The heating was done at an average rate of 2 °C min^{-1}. The material after the calcination process was crushed and ground in a ball mill to a fineness below 63 μm and again pressed under 80 MPa. All the pressed samples were sintered at 1500 °C and a soaking period of 30 h at the designed temperature. The as-obtained product was ball-milled to form powder. Additionally, industrial reactive alumina (PFR, Alteo) was also used as a raw material.

Hydrated paste samples preparation and test methods

The hydraulic behavior of $Ca_7ZrA_6O_{18}$ as well as of the mixtures of $Ca_7ZrA_6O_{18}$ with reactive alumina was investigated by differential calorimetric analysis and other methods. The investigated mixtures were 75 mass% $Ca_7ZrA_6O_{18}$/25 mass% Al_2O_3, 50 mass% $Ca_7ZrA_6O_{18}$/50 mass% Al_2O_3 and 25 mass% $Ca_7ZrA_6O_{18}$/75 mass% Al_2O_3. The single component samples were 100 mass% $Ca_7ZrA_6O_{18}$ and 100 mass% Al_2O_3. To further simplify the notation, individual oxides are abbreviated as a single letter, i.e., $C \equiv CaO$, $A \equiv Al_2O_3$, $Z \equiv ZrO_2$ and $H \equiv H_2O$. Hydrated paste samples were prepared as follows: The following reagents in the given proportions were homogenized together and then mixed with water to produce pastes which were cured in a climatic chamber at 20 and 50 °C for 32 days at 90 % relative humidity (RH). The obtained samples were denoted as $100C_7A_3Z$-H-T20, 25A-75C_7A_3Z-H-T20, 50A-50C_7A_3Z-H-T20 and 75A-25C_7A_3Z-H-T20 (cured at 20 °C) and $100C_7A_3Z$-H-T50, 25A-75C_7A_3Z-H-T50, 50A-50C_7A_3Z-H-T50 and 75A-25C_7A_3Z-H-T50 (cured at 50 °C). For use in XRD, FT-IR and DTA–TG tests, the cores of broken pastes were ground and treated with cold acetone to stop the hydration process. X-ray diffraction (XRD), differential thermal/thermogravimetric analysis (DTA–TG) and Fourier transform infrared spectroscopy (FT-IR) were performed to identify the phase composition of the fine powder samples. X-ray powder diffraction (XRD) patterns were obtained on a X'Pert Pro PANalytical X-ray diffractometer. The XRD patterns of previously synthesized material, reactive alumina and acetone quenched hydrated powdered samples were collected by step scanning with step of 0.02 degree over the range 5°–90° at room temperature. The specific surface and grain size distribution of the synthesized $Ca_7ZrAl_6O_{18}$ material were measured by a laser diffraction analyzer (Master Sizer 2000 version 5.60 apparatus of Malvern, UK).

DTA–TG was carried out using an NETZSCH STA 449 F3 Jupiter thermal analyzer. The temperature was programmed to rise at a constant heating rate of 10 °C min^{-1} up to 1000 °C. The test was performed under an air flow of 40 mL min^{-1}. A Bruker Vertex 70v spectrometer was used for studying the curing of the $Ca_7ZrAl_6O_{18}$ and reactive alumina/$Ca_7ZrAl_6O_{18}$ pastes. The FT-IR spectrometer was operated in the mid-IR region (4000–400 cm^{-1}) with a

resolution of 4 cm^{-1}. Each spectrum was the average of 128 scans. Samples were prepared by the standard KBr pellet method. The morphologies of the binder pastes were observed through using scanning electron microscope FEI Nova NanoSEM 200. For the analysis, freshly broken surfaces were prepared without hydration interruption before observation and coated with carbon.

Hydration heat of $100C_7A_3Z$, 25A-$75C_7A_3Z$, 50A-$50C_7A_3Z$, 75A-$25C_7A_3Z$ and 100A with water-to-solid ratio of 0.5 was measured by the differential non-isothermal–non-adiabatic calorimeter. The homogenized pastes of binders and water were prepared by an intensive mixing in a beaker for 1 min at 20 °C, and the obtained samples were immediately put into the calorimeter. The hydration reaction was carried out with the initial hydration temperature of 20 °C.

Results and discussion

Characterization of starting materials

High-purity commercial mono-modal reactive alumina powder (PFR, $d_{50} = 0.5$ μm) from Alteo was used as raw material. XRD results showed that no peaks except α-alumina (corundum) were found in the XRD spectra. Particle size distribution of the synthesized calcium zirconium aluminate revealed the most of the powder is in micron level and around 50 vol% of the material was below 21 μm. The XRD study obtained from the synthesized sample revealed that $Ca_7ZrAl_6O_{18}$ was identified as the major crystalline phase as well as very small peaks related to impurity of $CaZrO_3$.

Calorimetric studies

The heat evolved values versus curing time are given in Table 1, the heat evolved $Q(t) = f(t)$ is shown in Fig. 1, and the heat evolution curves $dQ/dt = f(t)$ are shown in Fig. 2. The kinetics of hydration of the binders is shown in Fig. 2. The figure shows the rates of heat liberation (dQ/dt) during the first 12 h after mixing with water as a function of temperature. The calorimetric curves shown in Fig. 2 exhibit one major feature, i.e., an intense heat peak, which occurs immediately after mixing with water. This peak is referred to hydration of $Ca_7ZrAl_6O_{18}$ when present alone ($100C_7A_3Z$) or in admixture with reactive Al_2O_3 micropowder (25A-$75C_7A_3Z$, 50A-$50C_7A_3Z$, 75A-$25C_7A_3Z$) and is associated with both wetting and reaction in which an anhydrous solid is converted to the hydration products [14]. The reason for this is because the calorimetric curve of alumina (100A) has only a mixing peak due to the initial wetting of the powder. The high heat evolution, accompanying the formation of hexagonal hydrates, raises the temperature of the hydrating binders appreciably. It would be reasonable to assume that the acceleration effect temperature on the conversion reaction of these hydrates to cubic hydrate (C_3AH_6) will occur. As shown in Fig. 1 and Table 1, with increase in reactive Al_2O_3 micropowder in the binder mass, the total amount of heat released during hydration decreases considerably. Nevertheless, the presence of reactive alumina in the binder mass can facilitate the heterogeneous nucleation of C–A–H phases.

Table 1 The total amount of heat released during hydration of binders versus curing time in J g^{-1}

Binder	Curing time / h					
	0.5	1	2	4	8	12
$100C_7A_3Z$	182	248	294	329	360	379
25A_$75C_7A_3Z$	150	201	239	268	294	310
50A_$50C_7A_3Z$	116	156	186	206	224	234
75A_$25C_7A_3Z$	92	119	135	145	151	154
100A	42	47	48	48	48	48

X-ray diffraction (XRD) analysis of hardened binder pastes

Figures 3 and 4 show the XRD patterns of the hardened binder pastes without ($100C_7A_3Z$-H) and with reactive alumina powder (25A-$75C_7A_3Z$-H, 50A-$50C_7A_3Z$-H, 75A-$25C_7A_3Z$-H) cured at 20 and 50 °C, respectively. It is observed that the products obtained by hydration of $Ca_7ZrAl_6O_{18}$ at 20 °C are amorphous in nature and are characterized by the low-intensity XRD peaks; however, by

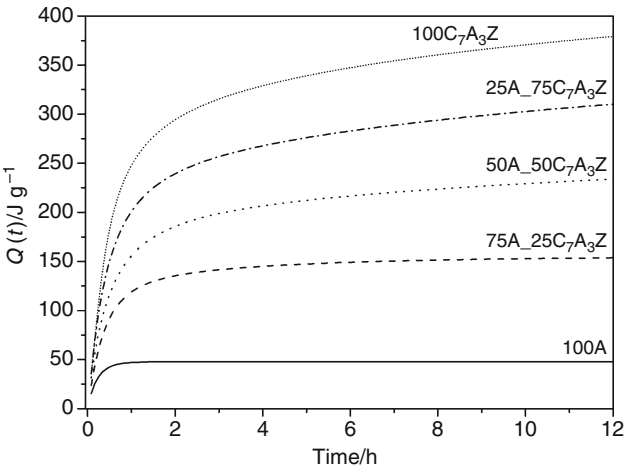

Fig. 1 Plots showing total heat evolution in J g^{-1} at 20 °C as a function of time for the first 12 h of hydration of reactive alumina, calcium zirconium aluminate and their binary mixtures

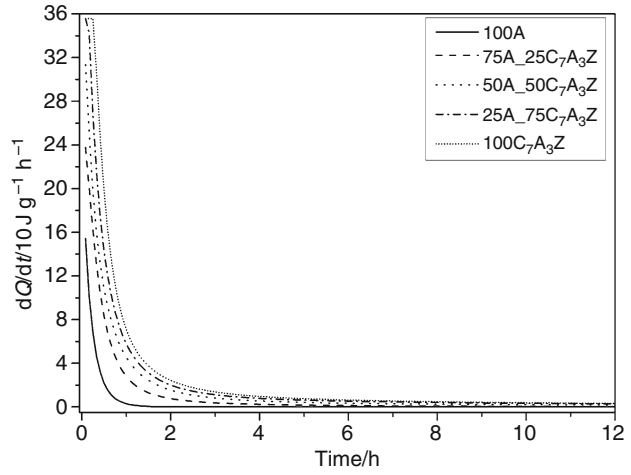

Fig. 2 Calorimetric curves plotting the rates of heat evolution in J g^{-1} h^{-1} by reactive alumina, calcium zirconium aluminate and their binary mixtures as a function of time when reacted with water for 12 h at 20 °C

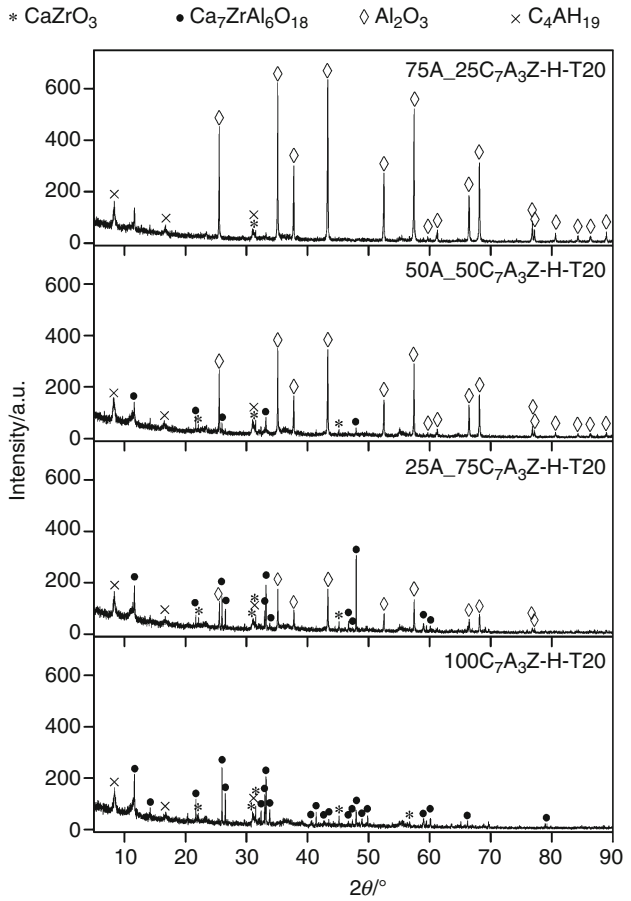

Fig. 3 X-ray diffraction patterns of $Ca_7ZrAl_6O_{18}$ without ($100C_7A_3Z$-H-T20) and with reactive alumina (25A-$75C_7A_3Z$-H-T20, 50A-$50C_7A_3Z$-H-T20, 75A-$25C_7A_3Z$-H-T20) and hydrated for 32 days at 20 °C

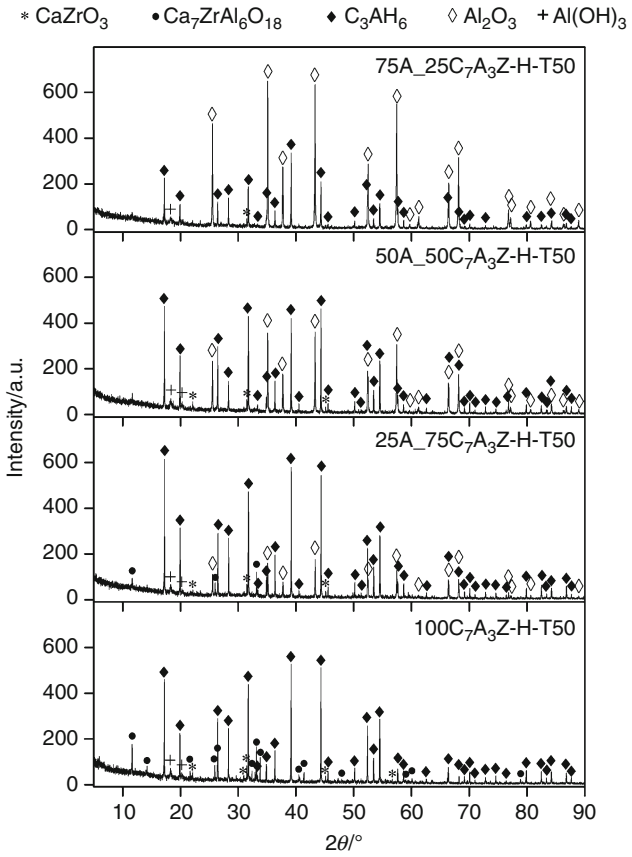

Fig. 4 X-ray diffraction patterns of $Ca_7ZrAl_6O_{18}$ without ($100C_7A_3Z$-H-T50) and with reactive alumina (25A-$75C_7A_3Z$-H-T50, 50A-$50C_7A_3Z$-H-T50, 75A-$25C_7A_3Z$-H-T50) and hydrated for 32 days at 50 °C

XRD analysis were detected new peaks corresponding to tetracalcium aluminate hydrate, C_4AH_{19} (Fig. 3). The quite broadened and low-intensity XRD peaks all suggest that C_4AH_{19} is rather poorly crystalline. With increasing curing temperature at 50 °C, intense C_3AH_6 peaks were found, due to the high crystallinity of this phase after the thermal treatment. It is observed that $Al(OH)_3$ is not amorphous in nature and characterized by the sharp peaks (Fig. 4). Different hydration degrees were seen for the hardened binder pastes cured at 20 and 50 °C (Figs. 3, 4). Absence of any major peak belonging to $Ca_7ZrAl_6O_{18}$ suggests that transformation of this phase is complete in the hardened binder paste containing 50 mass% Al_2O_3 cured at 50 °C (50A-$50C_7A_3Z$-H-T50), while at the lower curing temperature remains present in the unhydrated form (50A-$50C_7A_3Z$-H-T20) (Figs. 3, 4). The unhydrated $Ca_7ZrAl_6O_{18}$ residue could be explained by a surface coverage of the binder grains by early hydration, which impeded further $Ca_7ZrAl_6O_{18}$ hydration. Nevertheless, no dormant period caused by a hydrated layer was occurred in the heat

evolution curves (Fig. 2), as shown by previous calorimetry studies. $Ca_7ZrAl_6O_{18}$ reacted with water, forming calcium aluminate hydrates and its accompanying hydration products, i.e., the different forms of aluminum hydroxide and $CaZrO_3$ [14–17]. Free α-Al_2O_3 was also detected in the hardened binder pastes by XRD and becomes dominant with increasing the content of reactive alumina.

Spectroscopic analysis (FT-IR) of hardened binder pastes

IR analysis was applied to supplement XRD data and more fully characterize hydration products formed in the hardened binder pastes [20]. It was capable of differentiating poorly crystalline amorphous calcium aluminate hydrates as readily as crystalline phases which was a limitation of XRD method, beside C_4AH_{19} and C_3AH_6 previously found in XRD measurements. The FT-IR spectra of the hydrated $Ca_7ZrAl_6O_{18}$ without and with reactive alumina cured at 20 and 50 °C are shown in Figs. 5 and 6, respectively. The spectra of hydrated pastes prepared using different curing temperatures showing different absorption bands indicate not the same hydration products for these samples. FT-IR spectra of at ambient temperature metastable hydrates, CAH_{10}, C_2AH_8 and C_4AH_{19} showed similarities, as hexagonal plate-type structure, usually overlapped if more than one hexagonal hydrates coexist, but these were considerably different from the spectra of the hydrogarnet or cubic phase (C_3AH_6).

The FT-IR spectra of the hydrated pure $Ca_7ZrAl_6O_{18}$ paste and cured at 20 °C ($100C_7A_3Z$-H-T20) allowed identification of the hexagonal hydrates CAH_{10}, C_2AH_8 and C_4AH_{19}. Broad band in the absorption range of 4000–3000 cm^{-1} was due to the O–H groups in calcium aluminate hydrates and alumina gel. The IR spectra of CAH_{10} have a very broad and intense band due to hydroxyl vibration in the 3550–3400 cm^{-1} region, with maxima located near to 3500 cm^{-1}. The peaks located at 3622, 3528, 3472, 1645, 584, 534 and 420 cm^{-1} were probably due to C_2AH_8 [21], but some of these absorption bands supported the assumption of the presence of C_4AH_{19} hydrate. Aruja [22] discussed the solid solution formation between tetracalcium aluminate hydrate and di-calcium aluminate hydrate. Hence, it is difficult to specify the characteristic vibration bands of C_4AH_{19}. A very weak band at 1645 cm^{-1} corresponding to H_2O deformation mode supported the evidence for the presence of hexagonal hydrates. This is the main difference between cubic phase and the hexagonal ones. The IR spectra also present OH-free band at 3676 cm^{-1} due to the formation of stable C_3AH_6 phase. Others fundamental bands due to the stretching and bending vibrations of the Al–O in the AlO_6 groups appearing at about 802, 525 and 412 cm^{-1} identified in the Ref. [23, 24] could overlap with the hexagonal phase absorption bands presented in our experimental spectrum. Nevertheless, the strong band

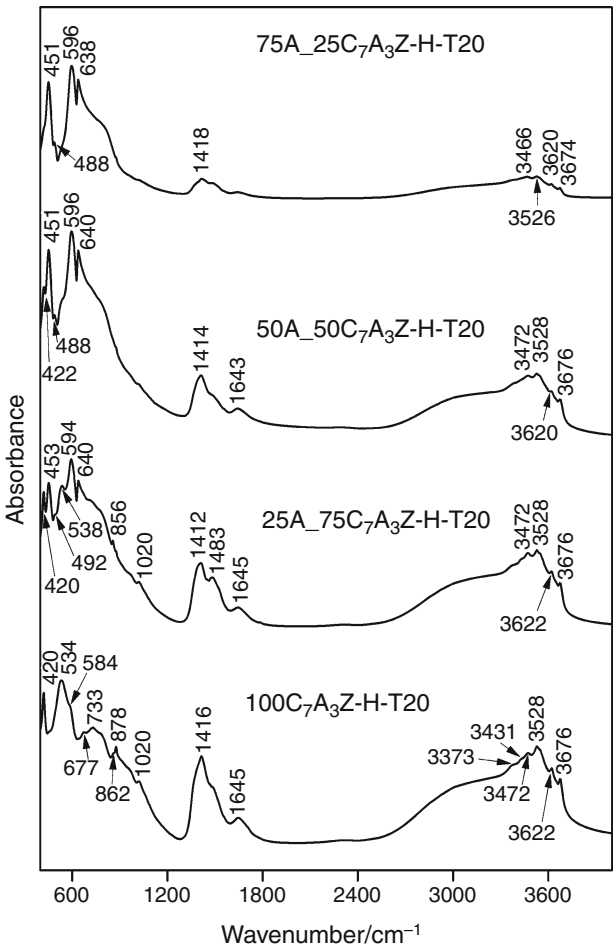

Fig. 5 FT-IR spectra of the hydrated form of $Ca_7ZrAl_6O_{18}$ and hydrated binary mixtures of $Al_2O_3/Ca_7ZrAl_6O_{18}$ cured at 20 °C

at about 534 cm^{-1} appearing in the spectrum Fig. 5 is an essentially "pure" or "isolated" AlO_6 octahedra vibration [25]. According to FT-IR analysis results, it was confirmed that both the hexagonal and cubic hydration products coexist under these conditions. It has been clearly shown that these results are in good agreement with the microcalorimetric results. The heat generated by the $Ca_7ZrAl_6O_{18}$ hydration has raised the temperature of pastes and accelerated conversion reaction causing coexistence of both unstable calcium aluminate hydrates and thermodynamically more stable C_3AH_6. Moreover, the absorption peaks appearing at 3622, 3528 and 3472 cm^{-1} due to O–H stretching vibration in gibbsite supported the evidence for the presence this compound. Another gibbsite bands, i.e., 1020 cm^{-1} coming from O–H bending vibration and at 534 cm^{-1} due to AlO_6 vibration, are in very good agreement with that found in the literature [23, 25]. It was found that both hexagonal and cubic hydration products are susceptible to carbonation and can react with atmospheric CO_2. The stretching vibrations of CO_3^{2-} in carbonates were observed at 1416 cm^{-1} (Fig. 5). The bands at 878 and

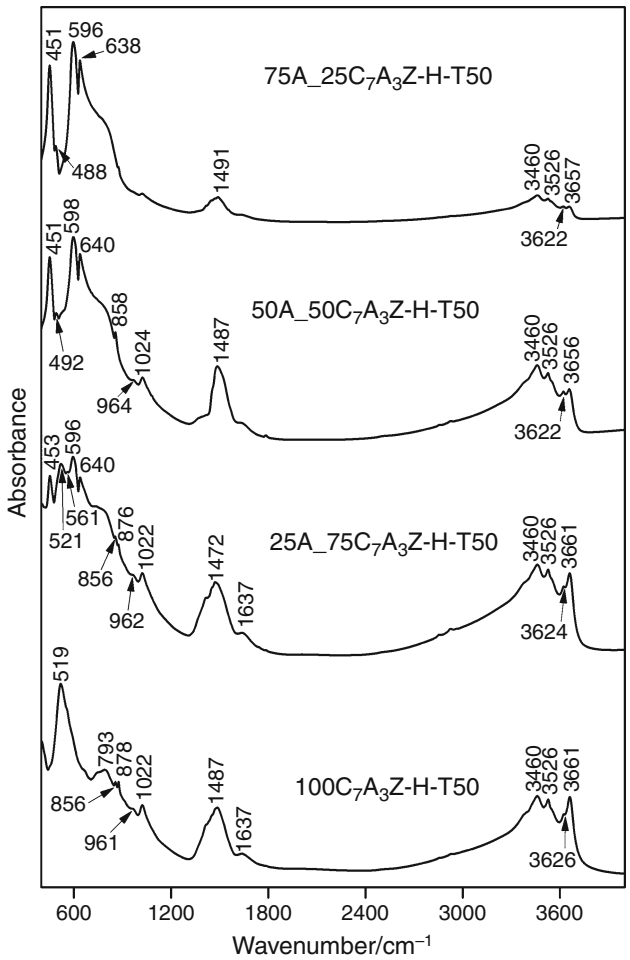

Fig. 6 FT-IR spectra of the hydrated form of $Ca_7ZrAl_6O_{18}$ and hydrated binary mixtures of $Al_2O_3/Ca_7ZrAl_6O_{18}$ cured at 50 °C

862 cm^{-1} are also calcium carbonate bands. The presence of a broad band centered at 733 cm^{-1} confirmed that still some unhydrated $Ca_7ZrAl_6O_{18}$ was also present. In mixtures reactive alumina/$Ca_7ZrAl_6O_{18}$ cured at 20 °C (25A-75C_7A_3Z-H-T20, 50A-50C_7A_3Z-H-T20, 75A-25C_7A_3Z-H-T20), the modes corresponding to the α-Al_2O_3 coexisting with calcium aluminate hydrates can be identified. According to Tarte [25], the most characteristic feature of the IR spectrum of corundum being the strong absorption bands near 650 and 600 cm^{-1}. The IR spectrums of systems with reactive alumina contain absorption band at about 453, 492, 594 and 640 cm^{-1} caused by α-Al_2O_3 (Fig. 5). The absorption bands observed in the ranges 4000–3000 and 1750–1580 cm^{-1} considered as the characteristic peaks of hexagonal calcium aluminate hydrates gradually disappeared with increasing reactive alumina content (25A-75C_7A_3Z-H-T20, 50A-50C_7A_3Z-H-T20, 75A-25C_7A_3Z-H-T20—Fig. 5). Also, the hydrated $Al_2O_3/Ca_7ZrAl_6O_{18}$ mixtures were less susceptible to the carbonation process due to decreasing the amount of C–A–H phases.

The shapes of FT-IR spectra for the hydrated $Ca_7ZrAl_6O_{18}$ without and with reactive alumina cured at 50 °C (Fig. 6) are noticeably different. They clearly show that at high temperature, noticeable sharpening of the bands occurs. The strong sharp bands appearing in the 3670–3400 cm^{-1} are due to valence OH vibrations of the water molecules in the cubic C_3AH_6 hydrate and aluminum hydroxide, $Al(OH)_3$. The strong peaks at 3661 and additionally at 519 cm^{-1} correspond to C_3AH_6, which was formed when calcium zirconium aluminate was subjected to hydration reaction at elevated temperature (50 °C). The 3665 cm^{-1} band is distinctive for this phase while the strong 519 cm^{-1} can be assigned to the vibration of AlO_6 group in the hydrogarnet structure [25]. Considering the data from spectra collected during the present investigation, it was possible to indicate the absorption bands of aluminum hydroxide, gibbsite at 3626, 2526, 3460, 1022 and 961 cm^{-1}. The broad peak located at 793 cm^{-1} supported the presence of unhydrated $Ca_7ZrAl_6O_{18}$ in the hydrated pure paste. In the spectra for the hydrated pure $Ca_7ZrAl_6O_{18}$ (100C7A3Z-H-T50) and the $Al_2O_3/Ca_7ZrAl_6O_{18}$ mixture containing 25 mass% reactive alumina (25A-75C_7A_3Z-H-T50) (Fig. 6), there is a peak at 1637 cm^{-1} caused by the H–O–H deformation band and provides spectroscopic evidence of the presence of secondary hexagonal hydrates. Through IR spectroscopy, it can be seen that hydrated samples cured at 50 °C were also strongly affected by atmospheric CO_2.

Analysis of thermal dehydration of hardened binder pastes by DTA and TG

DTA–TG is considered one of the most powerful tools in the investigation of the hydration of CAC pastes [16, 26]. Curves have yielded useful results on the calcium zirconium aluminate hydrated for various lengths of time under different conditions [14–16]. Amorphous or poorly crystallized compounds not easily identifiable by XRD give characteristic thermal peaks. Curves of the $Ca_7ZrAl_6O_{18}$ and the mixtures $Ca_7ZrAl_6O_{18}$/reactive Al_2O_3 for 32 days at 20 °C and even at elevated temperatures (50 °C) obtained in this study are shown in Figs. 7 and 8. DTA curves of $Ca_7ZrAl_6O_{18}$ without and with reactive alumina cured at 20 °C (Fig. 7) show three endothermic effects corresponding to the stepwise dehydration of pastes. There are some differences regarding the type of calcium aluminate hydrates that forms initially in $Ca_7ZrAl_6O_{18}$ paste, as it has been discussed in Ref. [14]. The results do not seem to be consistent, and much more systematic work is needed to establish the products in the all stages of hydration of $Ca_7ZrAl_6O_{18}$ at 20 °C. The CAH_{10} decomposed at 88 °C was reported to be the preferred product. The 32-day hydrated compound (100C_7A_3Z-H-T20) gives three peaks at 123, 188 and 293 °C due to the stepwise dehydration of

both amorphous and crystalline hydration products AH_3-gel, CAH_{10}, C_2AH_8, C_4AH_{19}, $Al(OH)_3$ and C_3AH_6. Ukrainczyk et al. [21] found three endothermic effects corresponding to the stepwise dehydration of C_2AH_8 at about 110, 175 and 300 °C. The thermal effect at about 120 °C in hydrated pastes in of great interest in the interpretation also dehydration reaction of CAH_{10}. The endothermic peak below this temperature may be partially due to the presence of the amorphous AH_3-gel. The two endothermic effects at 188 and 293 °C (Fig. 7) occur very close to the hexagonal phase studied by Ramachandran and Feldman [27] showing two typical endothermal peaks at 195 and 280 °C owing to dehydration of C_2AH_8 and C_4AH_{13}, respectively. Considerations on the stability in the system $CaO–Al_2O_3–H_2O$ conducted by Lothenbach et al. [28] indicate that at ≥88 %, relative humidity C_4AH_x is stable as C_4AH_{19} but dehydrates to C_4AH_{13} at ≤81 % relative humidity. C_4AH_{19} is also considered as phase structurally derived from C_4AH_{13} hydrate by the addition of an extra layer of H_2O molecules. It should be noted that the structural changes of crystalline C_4AH_{19} (Fig. 3) probably occurred with increasing temperature during the DTA–TG measurement and the C_4AH_{19} phase dehydrates to the C_4AH_{13} phase during this drying procedure. An endothermic peak at about 293 °C represented the presence of the remainder C_4AH_{13}. This DTA peak may be also due to the formation of $Al(OH)_3$. The mixtures reactive Al_2O_3/$Ca_7ZrAl_6O_{18}$ which had been hydrated at 20 °C indicated endothermic effects for the expulsion of water at the same temperatures found for the hydrated $Ca_7ZrAl_6O_{18}$ (Fig. 7). Only, the shift in the first peak temperature may be due to the presence of AH_3-gel that forms initially in the reaction of fine-particle alumina and water. Recrystallization of dehydrated calcium aluminates was manifested by sharp exothermic reaction in the range 920–950 °C in the mixtures of Al_2O_3/$Ca_7ZrAl_6O_{18}$ (Fig. 7). It was concluded that in pastes of Al_2O_3/$Ca_7ZrAl_6O_{18}$, reactive alumina favor the nucleation and crystallization of calcium aluminates.

The pastes cured for 32 days at 50 °C exhibited an endothermic effect at about 320–340 °C (Fig. 8) which was attributed to dehydration of the binder phase C_3AH_6. The formation of stable cubic phase (hydrogarnet) by the

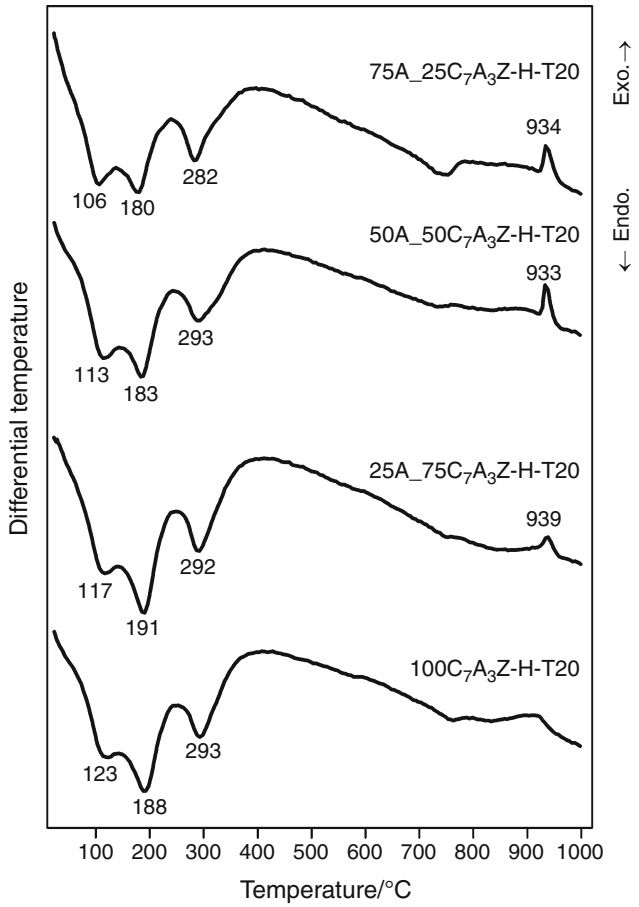

Fig. 7 DTA curves of $Ca_7ZrAl_6O_{18}$ without ($100C_7A_3Z$-H-T20) and with reactive alumina (25A-$75C_7A_3Z$-H-T20, 50A-$50C_7A_3Z$-H-T20, 75A-$25C_7A_3Z$-H-T20) and hydrated for 32 days at 20 °C

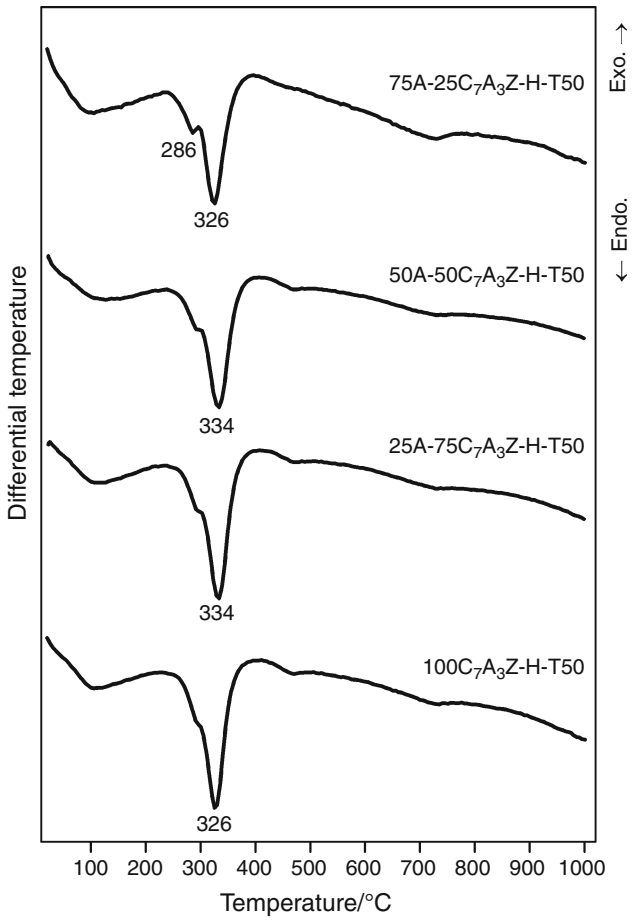

Fig. 8 DTA curves of $Ca_7ZrAl_6O_{18}$ without ($100C_7A_3Z$-H-T50) and with reactive alumina (25A-$75C_7A_3Z$-H-T50, 50A-$50C_7A_3Z$-H-T50, 75A-$25C_7A_3Z$-H-T50) and hydrated for 32 days at 50 °C

interaction of $Ca_7ZrAl_6O_{18}$ with water at 60 °C has been studied in the literature [15]. Nevertheless, the DTA curves presented in this paper showed that the endothermic peaks shift toward higher temperature. The mixes different in reactive alumina content formed a more ordered cubic phase C_3AH_6. The possibility of influence of alumina on the nucleation process of the hydrates has received some attention in recent years [29, 30]. This is particularly evident for the paste with 75 mass% Al_2O_3 (Fig. 8) where an additional endothermic peak at 286 °C representing the presence of $Al(OH)_3$ is observed.

SEM/EDS observations of hardened binder pastes

Addition of reactive alumina influences both the hydration behavior of $Ca_7ZrAl_6O_{18}$ in binder systems, as previously highlighted in XRD, FT-IR, DTA–TG discussion, and morphology of the formed hydrated products of hardened binder pastes (Figs. 9, 10). Figures 9a and 10a present SEM micrographs of neat $Ca_7ZrAl_6O_{18}$ pastes hydrated at 14 days at 20 and 50 °C, respectively. Figures 9b and 10b showed SEM micrographs of hardened $Ca_7ZrAl_6O_{18}$ pastes containing 25 mass% reactive Al_2O_3 hydrated for 14 days at 20 and 50 °C, respectively. Figure 9a showed that the micrograph is composed of dense structure of amorphous gel and poorly crystalline hexagonal calcium aluminate hydrates. The micrograph of $Ca_7ZrAl_6O_{18}$ paste containing of fine Al_2O_3 particles cured under sealed conditions at 20 °C (Fig. 9b) indicates that a large amount of more crystalline form of C–A–H phase was formed. In Fig. 10a, one can observe a very dense structure in the hardened matrix. The main hydration products of the $Ca_7ZrAl_6O_{18}$ matrix formed at 50 °C are fully crystalline hydrates C_3AH_6 and $Al(OH)_3$ having close structure. Figure 10b shows a mixture of well-crystalline hydration products and calcium hydroaluminate binding phase formed in the hardened $Ca_7ZrAl_6O_{18}$ paste containing 25 mass% reactive alumina. SEM results show that considerable amounts of amorphous products were produced, especially during the hydration of both the $Ca_7ZrAl_6O_{18}$ phase at 20 °C and the $Ca_7ZrAl_6O_{18}$/reactive Al_2O_3 mixtures cured at 50 °C.

Conclusions

1. The hydration heat of the binder containing reactive alumina is smaller than that of the mono-phase hydraulic binder based on calcium zirconium aluminate

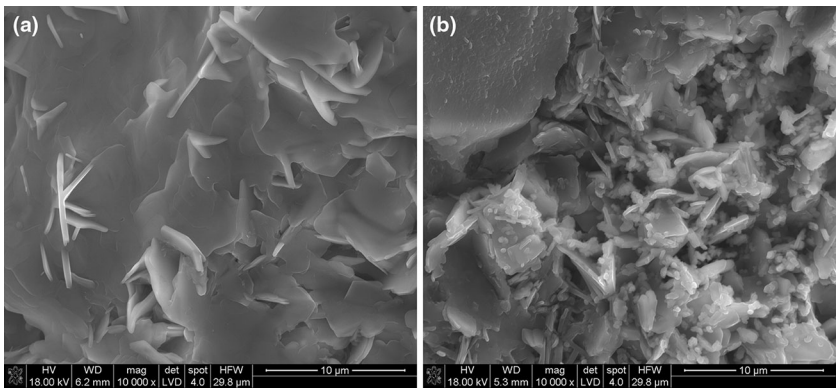

Fig. 9 Morphologies of hydrated $Ca_7ZrAl_6O_{18}$-based materials cured at 20 °C: **a** the reference, **b** $Ca_7ZrAl_6O_{18}$ containing 25 mass% reactive alumina

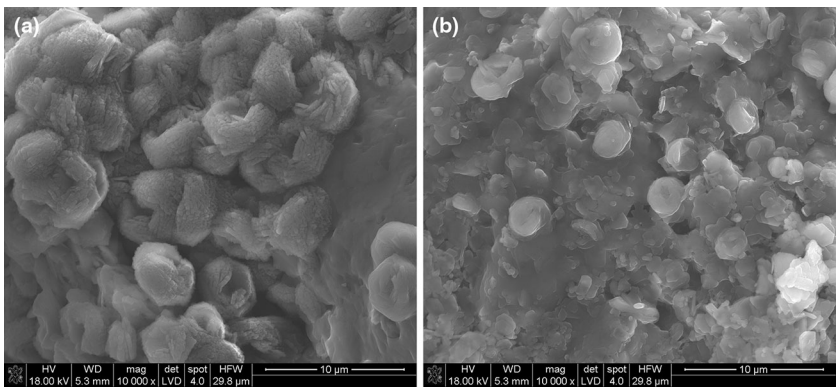

Fig. 10 Morphologies of hydrated $Ca_7ZrAl_6O_{18}$-based materials cured at 50 °C: **a** the reference, **b** $Ca_7ZrAl_6O_{18}$ containing 25 mass% reactive alumina

($Ca_7ZrAl_6O_{18}$) while binding properties of the two-component binder systems were maintained.

2. Curing temperature affected the hydration products formed in the hydration products of both $Ca_7ZrAl_6O_{18}$ and $Ca_7ZrAl_6O_{18}/Al_2O_3$ blends greatly. At the curing temperature 20 °C, X-ray amorphous hydrates were mainly formed during the $Ca_7ZrAl_6O_{18}/Al_2O_3$ binder's hydration process and the water-rich calcium aluminate hydrate, i.e., C_4AH_{19} was the only detected crystalline hydration product. At the elevated curing temperature 50 °C, the formation of predominant crystalline $Al(OH)_3$ and the C_3AH_6 phases occurred.
3. Aluminum oxide micropowder influences the hydration behavior of $Ca_7ZrAl_6O_{18}$ facilitating the nucleation and growth of hydration products and lead also to differences in the microstructure of the hardened pastes. It may be concluded based on DTA measurement that reactive alumina favored also recrystallization of dehydrated calcium aluminates.
4. Accompanying hydration products, i.e., refractory binary compound—calcium zirconate, $CaZrO_3$, was detected at both 20 °C and elevated curing temperatures.
5. Hence, due to this unique combination of properties, $Ca_7ZrAl_6O_{18}/Al_2O_3$ binders can be used in many types of new refractories including unshaped mixtures.

Acknowledgements This work is supported by the Grant No. INNOTECH-K2/IN2/16/181920/NCBR/13 of the National Centre for Research and Development.

References

1. Singh VK. High-alumina refractory castables with calcium aluminate binder. J Mater Sci Lett. 1989;8:424–6.
2. Sakai E, Sugiyama T, Saito T, Daimon M. Mechanical properties and micro-structures of calcium aluminate based ultra high strength cement. Cem Concr Res. 2010;40(6):966–70.
3. Silva AP, Segadães AM, Pinto DG, Oliveira LA, Devezas TC. Effect of particle size distribution and calcium aluminate cement on the rheological behaviour of all-alumina refractory castables. Powder Technol. 2012;226:107–13.
4. Obradović N, Terzić A, Pavlović L, Filipović S, Pavlović V. Dehydration investigations of a refractory concrete using DTA method. J Therm Anal Calorim. 2012;110(1):37–41.
5. Sawków J, Nocuń-Wczelik W. Calorimetric studies of refractory corundum. Calcium aluminate composites. J Therm Anal Calorim. 2003;74:451–8.
6. Nouri-Khezrabad M, Braulio MAL, Pandolfelli VC, Golestani-Fard F, Rezaie HR. Nano-bonded refractory castables. Thermochim Acta. 2013;39(4):3479–97.
7. Zhou N, Hu S, Zhang S. Advances in modern refractory castables. China's Refract. 2004;13(2):3–12.
8. Gogtas C, Lopez HF, Sobolev K. Role of cement content on the properties of self-flowing Al_2O_3 refractory castables. J Eur Ceram Soc. 2014;34:1365–73.
9. Gürel SB, Altun A. Reactive alumina production for the refractory industry. Powder Technol. 2009;196:115–21.
10. Ma W, Brown PW. Mechanisms of reaction of hydratable aluminas. J Am Ceram Soc. 1999;82(2):453–6.
11. De Oliveira IR, Studart AR, Valenzuela FAO, Pandolfelli VC. Setting behavior of ultra-low cement refractory castables in the presence of citrate and polymethacrylate salts. J Am Ceram Soc. 2003;23(13):2225–35.
12. Taylor HFW. Cement chemistry. 2nd ed. London: Thomas Telford; 1997.
13. Bonsall SB. Cement-free refractory castable system for wet process pumping/spraying. Patent US5968602. United States; 1999.
14. Madej D, Szczerba J, Nocuń-Wczelik W, Gajerski R. Hydration of $Ca_7ZrAl_6O_{18}$ phase. Ceram Int. 2012;38(5):3821–7.
15. Madej D, Szczerba J, Nocuń-Wczelik W, Gajerski R, Hodur K. Studies on thermal dehydration of the hydrated $Ca_7ZrAl_6O_{18}$ at different water–solid ratios cured at 60 °C. Thermochim Acta. 2013;569(10):55–60.
16. Szczerba J, Madej D, Śnieżek E, Prorok R. The application of DTA and TG methods to investigate the non-crystalline hydration products of $CaAl_2O_4$ and $Ca_7ZrAl_6O_{18}$ compounds. Thermochim Acta. 2013;567(10):40–5.
17. Szczerba J, Madej D, Dul K, Bobowska P. $Ca_7ZrAl_6O_{18}$ acting as a hydraulic and ceramic bonding in the MgO–$CaZrO_3$ dense refractory composite. Ceram Int. 2014;40(5):7315–20.
18. Fukuda K, Iwata T, Nishiyuki K. Crystal structure, structural disorder, and hydration behavior of calcium zirconium aluminate, $Ca_7ZrAl_6O_{18}$. Chem Mater. 2007;19:3726–31.
19. Stoch P, Szczerba J, Lis J, Madej D, Pędzich Z. Crystal structure and ab initio calculations of $CaZrO_3$. J Eur Ceram Soc. 2012;32:665–70.
20. Torréns-Martín D, Fernández-Carrasco L, Blanco-Varela MT. Conduction calorimetric studies of ternary binders based on Portland cement, calcium aluminate cement and calcium sulphate. J Therm Anal Calorim. 2013;114(2):799–807.
21. Ukrainczyk N, Matusinovic T, Kurajica S, Zimmermann B, Sipusic J. Dehydration of a layered double hydroxide-C_2AH_8. Thermochim Acta. 2007;464:7–15.
22. Aruja E. The unit cell and space group of $4CaO{\cdot}Al_2O_3{\cdot}19H_2O$ polymorphs. Acta Crystallogr. 1961;14:1213–6.
23. Fernández-Carrasco L, Torrens-Martín D, Morales LM, Martínez-Ramírez S. Infrared spectroscopy in the analysis of building and construction materials. In: Theophanides T, editor. Infrared spectroscopy—materials science, engineering and technology, InTech; 2012. doi:10.5772/36186. http://www.intechopen.com/books/infrared-spectroscopy-materials-science-engineering-and-technology/infrared-spectroscopy-of-cementitious-materials. ISBN 978-953-51-0537-4.
24. Fernandez-Carrasco L, Vazquez T. Aplicación de la espectroscopía infrarroja al studio de cement aluminoso. Mater Constr. 1996;46(241):39–51.
25. Tarte P. Infra-red spectra of inorganic aluminates and characteristic vibrational frequencies of AlO_4 tetrahedra and AlO_6 octahedra. Spectrochim Acta A Mol Spectrosc. 1967;23(7):2127–43.
26. Pacewska B, Nowacka M. Studies of conversion progress of calcium aluminate cement hydrates by thermal analysis method. J Therm Anal Calorim. 2014;117(2):653–60.

27. Ramachandran VS, Feldman RF. Effect of calcium lignosulfonate on tricalcium aluminate and its hydration products. Matér Constr. 1972;5(2):67–76.
28. Lothenbach B, Pelletier-Chaignat L, Winnefeld F. Stability in the system $CaO–Al_2O_3–H_2O$. Cem Concr Res. 2012;42(12):1621–34.
29. Möhmel S, Geβner W. The influence of alumina reactivity on the hydration behaviour of mono calcium aluminate. Solid State Ion. 1997;101–103:937–43.
30. Rettel A, Seydel R, Gessner W, Bayoux JP, Capmas A. Investigations on the influence of alumina on the hydration of monocalcium aluminate at different temperatures. Cem Concr Res. 1993;23:1056–64.